

# A New Change Detection Algorithm for SAR Images

S.Q. Huang\*, D.Z. Liu, X.H. Cai

Xi'an Research Inst. of Hi-Tech, Hongqing Town, 710025, Xi'an, P. R. China

## Abstract

Speckle noise of Synthetic aperture radar (SAR) image and the azimuth sensitivity for imaging obstruct the interpretation and applications for SAR images. But it is very much remote sensing source because it can acquire data under all-day and all weather. Texture features reflect the spatial property of ground objects. If texture features change, in general the ground object does so. Therefore, this paper deep analyzes SAR image texture feature and proposes a new multi-temporal SAR image change detection algorithm, which is called by texture features fusion voting (TFFV) algorithm. Finally, the airborne SAR image data tests the method and experimental results indicate that the presented methods are feasible.

**Keywords:** SAR image; change detection; texture feature

## 1. Introduction

SAR is an active microwave coherent imaging radar, so it can acquire remote sensing data under all weather and all day, which can made up for the shortage of optics and infrared remote sensing. Therefore, it has been applied widely in civil and military fields [1][2]. SAR image change detection technique is to acquire ground object change information through SAR images of the same scene at different time and to further realize the qualitative or quantitative analysis of an object. It is a technology that aims at SAR image feature to found data analysis method and it is used to recognize the change of state for an object or phenomena. With the development of SAR image technology, multi-platform, multi-band, multi-polarization SAR image resources supply the advantage for SAR object change detections. At present, SAR image change detection has been become the issue of remote sensing research and has widely potential applications [3-7]. For example, it can be utilized to monitor and assess natural disaster such as earthquake, flood, mud and rock flow; it can be used to monitor and survey ocean resource, ocean environment and seaport; it can be used for monitoring and assessment to environmental change and pollution; it can realize continuous reconnaissance for battlefield area or key monitoring targets; it can be used for target battle damage assessment.

There are many SAR image change detection methods presented in recent ten years [8-11], but the field is still a focus, for the potential applications of SAR image change detection are very great. Multi-temporal remote sensing image change detection methods may be classified into two big types [12]: post-classification comparison method and direct comparison method. The direct comparison method main includes image gray difference method, image gray ratio method, image texture feature difference method, correlative

coefficient method, image regression method and canonical correlation method. The post-classification comparison method includes supervised and unsupervised classifications. Each SAR image change detection method has its advantage and disadvantage. Even the multi-temporal SAR image comes from the same area, but if the applied approach is different, the detected results are different, and sometimes they are contrary. This is reason that every method tests the target area change from different aspects.

This paper proposes a novel multi-temporal SAR image change detection algorithm with the spatial texture feature of SAR images and some experiments are used to test the proposed algorithm and the experimental results show it effective.

## 2. The TFFV algorithm description

In SAR image change detection, it is insufficient to detect change only using image gray contrast, and the texture features information ought to be utilized to detect change. The texture features of an image describe the local mode of repeated appearance and their arrangement rule in image, which reflects some laws of gray change in macroscopy significance [13]. The usual definition of texture is some local properties of an image or a measurement of relation between local pixels. And image can be seen as the combination of different texture area. Texture features may be used to quantitatively describe space information of an image, and it is often related with the position, tendency, size and shape of an object, but it is independent of mean gray level. The texture of an image is not formalized, but it is relative with local gray and space organization.

There are eight statistic methods about image texture descriptions and measures, which are autocorrelation function, optimal transform, digital transform, textural edginess, structural element, gray-level cooccurrence matrix (GLCM), gray-level range and autoregressive model. In the following text, we mainly introduce the GLCM method. The GLCM emphasizes the spatial dependence of gray-level and the characteristic of it represents the spatial correlation of pixel gray under a sort of textural mode. The definition of GLCM is that each element  $(i, j)$  value in GLCM represents the frequency times of two pixels appearance under the pixel with value  $i$  occurred horizontally adjacent to a pixel with value  $j$ , neighbour distance value  $d$  and direction  $\alpha$  in a sliding window. Each element value of GLCM can be computed by next equation.

$$P(i, j) = \frac{p(i, j, d, \alpha)}{\sum \sum p(i, j, d, \alpha)} \quad (1)$$

In order to reduce the burden of computation, the gray scales of original image should be adjusted. In the general, the gray scales of most images are 256 levels. If we directly compute GLCM, it brings some difficulties. For a 256 levels

gray image, the size of GLCM is  $256 \times 256$  dimensions. But the texture features that we compute reflect the local characteristic of an image and it need not choose oversized window. There are large numbers of 0 values in  $256 \times 256$  GLCM and it becomes sparse matrix. In this way, on the one hand it does not represent textures well, on the other hand it also makes a great many of wasting of resources. Therefore, before the GLCM is created, image gray levels are processed in order to reduce the dimensions of GLCM. For SAR image, the gray levels are adjusted to 8 or 16 and it does not damage textural information basically [1]. Choosing the sliding window to compute GLCM is decided by image characteristics and extractive objects. That the size of window is small will ignore the correlation between pixels, which can not show the advantage of texture features. So the exactness ratio is lower when the size of window is small. With the window increasing, texture information gradually produces effect and the exactness ratio of change detection increases rapidly. When the size of window reaches some degree, the edge of image becomes blurring. It decreases the exactness of local image features and the pixel points of short distance bring confusion, which makes the exact ratio of change detection fall. The direction of GLCM little influences the computed value of characteristic quantity. The distance  $d$  usually only takes one or two in order that the textural measurement can be effectively connected with object features. The direction  $\alpha$  generally chooses four directions:  $0^\circ$ ,  $45^\circ$ ,  $90^\circ$  and  $135^\circ$ .

The GLCM can export a lot of texture features and their emphases are different, but many of them are relative. The TFFV change detection algorithm that is proposed by this paper, the algorithm chooses five relatively independent

textural features. They are the contrast feature, the energy feature, the correlation feature, the entropy feature and the homogeneity feature [14].

The TFFV algorithm is similar with the image gray difference algorithm. The difference is that the different pair of textural feature images can produce a difference map. When using texture difference algorithm detects change, what textural features are chosen for change detection is an important factor that decides the detection performance. The flow chart of the TFFV algorithm is shown in Fig.1, and the algorithm includes below steps.

(1) Gray levels demotion. In order to decrease the burden of computation, the original SAR images perform gray level demotion operations. In the TFFV algorithm, the gray level is demoted from 256 levels to 16 levels.

(2) Obtain the GLCM. Four GLCM are computed by Equation.(1) at four different directions which are  $0^\circ$ ,  $45^\circ$ ,  $90^\circ$  or  $135^\circ$  degree. They perform mean operations and the final GLCM is obtained.

(3) Obtain the single texture feature map. Because of choosing five texture features, which are contrast, energy, correlation, entropy and homogeneity, five texture feature maps will be obtained.

(4) Each feature map performs normalization processing. For original SAR image comes from different time, their intensity is different. In order to decrease errors, the feature maps should be performed normalization operations.

(5) Obtain the feature difference maps. After the feature maps are normalized, the corresponding feature maps perform the subtraction operation, and the corresponding feature difference maps are obtained.

(6) Obtain the changed map. Whether or not change of a

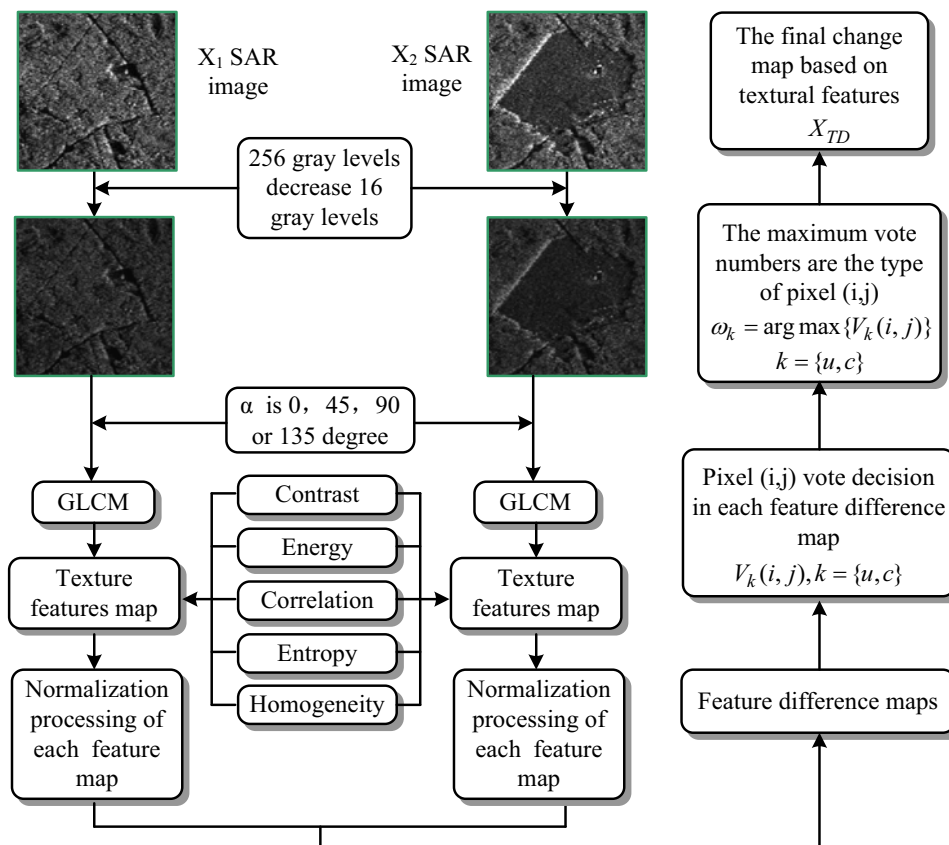


Fig.1 The flow chart of the TFFV algorithm

spatial position pixel  $(i, j)$  in all feature difference maps is decided by vote, and each element is an alternative: change  $\omega_c$  and no change  $\omega_u$ . The most vote numbers  $V_k(i, j), k = \{u, c\}$  that pixel  $(i, j)$  receives are acted as final classifications, namely, they are change type or no change type. They can be described by the next equation.

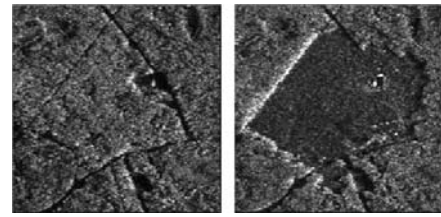
$$X_{TD}(i, j) \in \omega_k \Leftrightarrow \omega_k = \arg \max \{V_k(i, j)\} \quad (2)$$

Where  $k = \{u, c\}$ ,  $X_{TD}$  denotes the finale change map.

### 3. Experimental results and analysis

Suppose that the SAR images are  $X_1$  and  $X_2$  at different time  $t_1$  and  $t_2$ , respectively, and they are revised by radiation, geometry and registration. To verify the TFFV algorithm, using the gray difference method acts as comparative experiments. In experiments, the expectation maximization (EM) algorithm [15] is used to estimate the threshold. Experimental data adopts the remote sensing data of Canada centre for remote sensing airborne C/X-SAR. The original images are shown in Fig.2. Where, Fig.2(a) and Fig.2(b) are single-look SAR images at different time, which are C wave band HH polarization image and the space resolution is  $5m \times 5m$ . The imaging dates of Fig.2(a) and Fig.2 (b) are Mar. 18, 1991 and Feb. 8, 1992, respectively. Assume Fig.2(a) is  $X_1$  and Fig.2(b) is  $X_2$ . The area is a piece of forest. Because the frost is fallen, the ground object type takes place change, but its scattering structures don't change. This leads to final SAR image change. The scattering intensity of forest is stronger than that of bare ground surface. So after the forest is fallen, the backscattering intensity becomes weak. In SAR images, it indicates dark, which is shown in Fig.2(b). The brighter line area in the centre of Fig.2(b) is dihedral reflection effect between ground surface

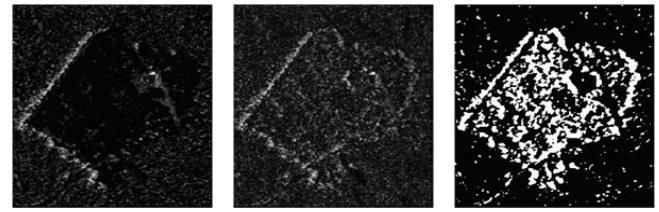
and forest. It belongs to strong scattering structure and the echo intensity is bigger, which is brighter in SAR image.



(a) Before change (b) After change

Fig.2 The SAR images before and after change

The change detected results with the gray difference algorithm are shown in Fig.3. Where, Fig.3(a) is the difference image  $X_D$  of  $X_2$  and  $X_1$ , namely,  $X_D = X_2 - X_1$ ; Fig.3(b) is the absolute value of  $X_D$ , i.e.  $|X_D|$ ; Fig.3(c) is the detected results with single threshold gray difference algorithm.



(a) (b) (c)

Fig.3 The detection results with gray difference method, (a) difference image, (b) the absolute values image of the difference image, (c) the results of change detection.

The change detection results with the TFFV algorithm are shown in Fig.4. Where, Fig.4(a) and Fig.4(b) are the images that the gray levels 256 are decreased into the gray

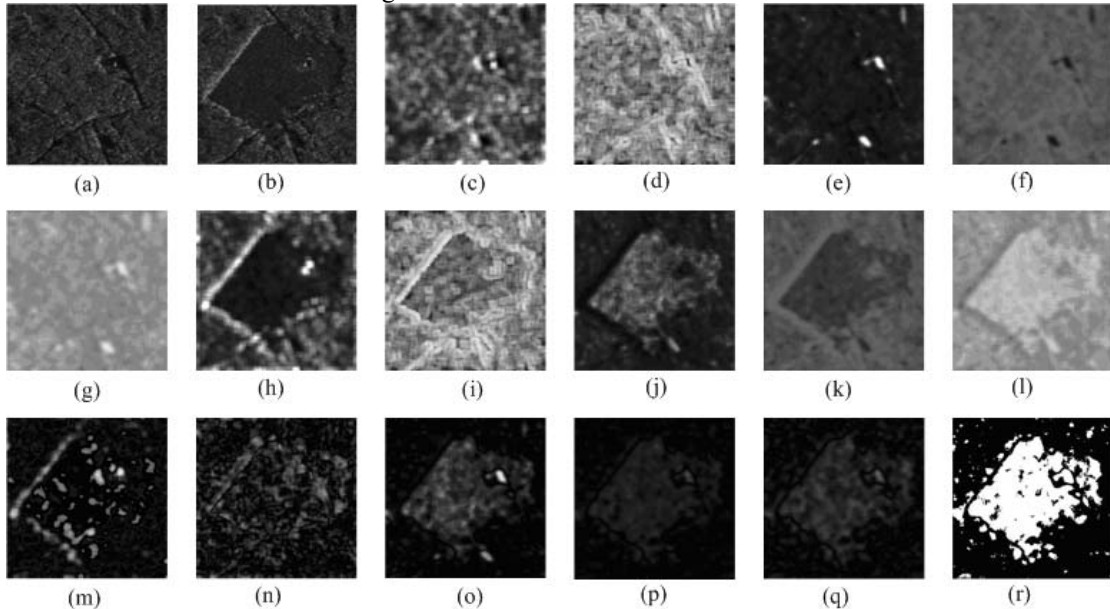


Fig.4 Textural features change detection,(a) 16 levels grey image of  $X_1$  image, (b) 16 levels grey image of  $X_2$  image, (c) contrast map of  $X_1$ , (d) correlation map of  $X_1$ , (e) energy map of  $X_1$ , (f) entropy map of  $X_1$ , (g) homogeneity map of  $X_1$ , (h) contrast map of  $X_2$ , (i) correlation map of  $X_2$ , (j) energy map of  $X_2$ , (k) entropy map of  $X_2$ , (l) homogeneity map of  $X_2$ , (m) detection results of contrast, (n) detection results of correlation, (o) detection results of energy, (p) detection results of entropy, (q) detection results of homogeneity, (r) detection results of the proposed texture feature fusion.

levels 16. Fig.4(c)-(g) and Fig.4(h)-(l) are the corresponding contrast map, correlation map, energy map, entropy map and homogeneity map of image  $X_1$  and  $X_2$ , respectively. Fig.4(m)-(q) are the detection result maps of the contrast map, correlation map, energy map, entropy map and homogeneity, respectively. Fig.4(r) is the detection results with the TFFV algorithm proposed by this paper.

#### 4. Conclusions

This paper studies the change detection method of multi-temporal SAR images from the spatial textural features, and proposes a new change detection algorithm called TFFV algorithm. Some real SAR image data performs comparative experiments between the gray difference method and the TFFV method. The experimental results show the proposed method is feasible. The future development of this work is how to reduce the influence that SAR image speckle noise brings to SAR image change detection.

#### References

- [1] H. D. Guo, "Radar for Earth Observation: Theory and Application", Beijing: Science Publishing House, 2000.
- [2] C. Oliver and S. Quegan, "Understanding Synthetic Aperture Radar Images", Artech House, Boston.London, 1998.
- [3] H. Skriver, M. T. Svendsen and A. G. Thomsen, "Multitemporal C- and L-band Polarimetric Signatures of Crops", IEEE Transactions on Geoscience and Remote Sensing, Vol. 37, No. 5, 1999, pp. 2413-2429.
- [4] H. Zhang, N. Hu, G. Liu, "Application of Multitemporal Composition and Classification to Land Use Change Detection", Geomatics and Information Science of Wuhan University, Vol. 30, No. 2, 2005, pp.131-134.
- [5] P. Gamba, F. Dell'Acqua and G. Trianni, "Rapid Damage Detection in the Bam Area Using Multitemporal SAR and Exploiting Ancillary Data", IEEE Transactions on Geoscience and Remote Sensing, Vol. 45, No. 6, 2007, pp.1582-1589.
- [6] S. Q. Huang, D. Z. Liu and L. Chen, "A study of the damage detection method for smooth earth surface", Acta Geophysica Sinica, Vol. 50, No. 4, 2007, pp. 315-321.
- [7] US Office Deal with Roadside Bomb with Unmanned Aerial Vehicle Synthetic Aperture Radar. <http://jczs.news.sina.com.cn/p/2006-11-05/0735409951.html>.
- [8] L. Castellana, A. D'Addabbo and G. Pasquariello, "A Composed Supervised/Unsupervised Approach to Improve Change Detection from Remote Sensing", Pattern Recognition Letters, Vol. 28, No.2, 2007, pp. 405-413.
- [9] F. Bovolo and L. Bruzzone, "A Detail-Preserving Scale-Driven Approach to Change Detection in Multitemporal SAR Images", IEEE Transactions on Geoscience and Remote Sensing, Vol. 43, No. 12, 2005, pp. 2963-2972.
- [10] L. Bruzzone and D. F. Prieto, "Automatic Analysis of the Difference Image for Unsupervised Change Detection", IEEE Transactions on Geoscience and Remote Sensing, Vol. 38, No. 3, 2000, pp. 1171-1182.
- [11] F. Chatelain, J. Y. Tournier and J. Inglada, "Change Detection in Multisensor SAR Images Using Bivariate Gamma Distributions," IEEE Transactions on Image Processing, vol.17, No.3, 2008, pp. 249-258.
- [12] D. Lu, P. Mausel, Z. E. Brondi, "Change Detection Techniques", International Journal of Remote Sensing, Vol. 25, No. 12, 2004, pp. 2365-2407.
- [13] Q. Q. Ruan, "Digital Image Processing", Beijing: Publishing House of Electronics Industry. 2001.
- [14] A. Baraldi and F. Parmiggiani, "An Investigation of the Textural Characteristics Associated with Gray Level Cooccurrence Matrix statistical Parameters", IEEE Transactions on Geoscience and Remote Sensing, Vol.33, No. 1, 1999, pp. 293-304.
- [15] T. K. Moon, "The Expectation-Maximization Algorithm", Signal Processing, Vol. 13, No. 6, 1996, pp. 47-60.